

See discussions, stats, and author profiles for this publication at: <https://www.researchgate.net/publication/245396067>

# Interaction among Ellipsoidal Inclusions and a Bimaterial Interface

Article in *JSME International Journal Series A* · April 2005

DOI: 10.1299/jsmea.48.100

---

CITATIONS

0

READS

15

3 authors, including:



**Nao-Aki Noda**

Kyushu Institute of Technology

695 PUBLICATIONS 3,769 CITATIONS

SEE PROFILE

# Interaction among Ellipsoidal Inclusions and a Bimaterial Interface\*

Nao-Aki NODA\*\*, Katsuya ONO\*\* and Yasuhiro MORIYAMA\*\*

Ellipsoidal inclusions can be regarded as a general model of defects in structures because they cover a lot of particular cases, such as line, circular and spherical defects. This paper deals with three-dimensional stress analysis for ellipsoidal inclusions in a bimaterial body under tension. The problem is formulated as a system of singular equations with Cauchy-type or logarithmic-type singularities, where unknowns are densities of body forces distributed in the  $r$ - and  $z$ -directions in bimaterial bodies having the same elastic constants of those of the given problem. In order to satisfy the boundary conditions along the ellipsoidal boundary, four types of fundamental density functions proposed in the previous paper are applied. Then the body force densities are approximated as a linear combination of fundamental density functions and polynomials. The present method is found to yield rapidly converging numerical results for stress distribution along the boundaries of both the matrix and inclusion even when the inclusion is very close to the bimaterial interface. Then, the effect of bimaterial surface on the stress concentration factor is discussed with varying the distance from bimaterial interface, shape ratio, and elastic modulus ratio.

**Key Words:** Elasticity, Stress Concentration, Body Force Method, Ellipsoidal Inclusion, Singular Integral Equation, Interaction

## 1. Introduction

Most engineering materials contain some defects in the form of cracks, voids or inclusions<sup>(1),(2)</sup>. To evaluate the defects on the strength of structures, it is necessary to know the stress concentration of those defects. As a model of defects elliptical and ellipsoidal inclusions are important because they cover a lot of particular cases, such as line, circular, and spherical defects. Previously, several researchers studied an ellipsoidal inclusion<sup>(3)–(6)</sup>, and discussed interactions among elliptical, and ellipsoidal inclusions<sup>(5)–(16)</sup>. Tsuchida et al. treated several elasticity problems of a spheroidal inclusion in a half-space<sup>(17)–(20)</sup>.

On the other hand, with increasing the use of composite materials in engineering structures, much attention has been paid to the strength of bimaterial interface. Since most materials contain some defects, it is essential to know the interaction among the defects and the interface. In the

previous studies, most researches have focused on fracture mechanics approach regarding interface<sup>(21)–(29)</sup>. In these cases, cracks in the vicinity of an interface have been assumed as a model of the defects after crack initiation and propagation. Little work has been done for the other model, especially for three-dimensional models before crack initiation. In this study, therefore, ellipsoidal inclusions of revolution near an interface are considered (see Fig. 1). Then, the interaction among the ellipsoidal inclusions and interface will be discussed.

## 2. The Proposed Model

In this paper, as shown in Fig. 1, three types of models will be considered. Then, the following notations will be used to describe the ellipsoidal inclusions with a bimaterial.

$E_{M1}, \nu_{M1}$  : Elastic modulus and Poisson's ratio of matrix 1

$E_{M2}, \nu_{M2}$  : Elastic modulus and Poisson's ratio of matrix 2

$E_{I1}, \nu_{I1}$  : Elastic modulus and Poisson's ratio of inclusion 1

$E_{I2}, \nu_{I2}$  : Elastic modulus and Poisson's ratio of inclusion 2

$a_i, b_i$  ( $i = 1, 2$ ) : Dimensions of the ellipsoidal inclusions

$d_i$  ( $i = 1, 2$ ) : Distance among the ellipsoidal inclusion and

\* Received 6th September, 2004 (No. 02-1435). Japanese Original: Trans. Jpn. Soc. Mech. Eng. Vol.69, No.684, A (2003), pp.1209–1215 (Received 13th December, 2001)

\*\* Department of Mechanical Engineering, Kyushu Institute of Technology, 1-1 Sensui-cho, Tobata, Kitakyushu 804-8550, Japan. E-mail: noda@mech.kyutech.ac.jp

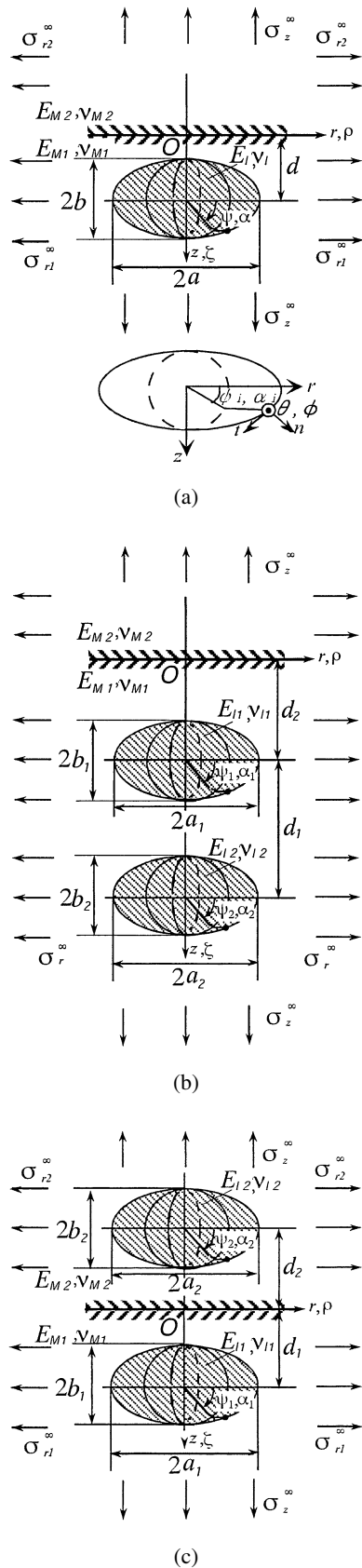


Fig. 1 Ellipsoidal inclusions in the vicinity of a bimaterial interface

interface

For example, in Fig. 1 (a), if the elastic ratio  $E_I/E_{M1} < 1$ , interface stresses  $\sigma_t$  in the matrix may cause crack initiation because they are larger than other stresses. Also, if  $E_I/E_{M1} > 1$ , interface stresses  $\sigma_n$  may cause interface debondings. If a crack initiates and propagates from the interface, the stress intensity factor is necessary to evaluate the strength of structures. Since little work has been carried out on the three-dimensional aspect, in our previous studies<sup>(30)–(32)</sup>, three-dimensional cracks near an interface have been treated in a similar way of the present solution.

In this study, the body force method<sup>(33)</sup> is used to formulate the elastic stress concentration problem of Fig. 1 as a system of singular integral equations. Then, the unknown body force densities are approximated by a linear combination of fundamental density functions and polynomials<sup>(34)–(36)</sup>. The present method gives smooth variations of interface stresses along the boundary.

### 3. Numerical Solutions

In the previous papers<sup>(34),(35)</sup>, numerical solutions of the singular integral equations of the body force method were discussed. Then, it was found that in the conventional body force method, unknown body force densities sometimes do not converge with increasing collocation points. To overcome this difficulty, eight fundamental densities were newly introduced<sup>(34),(35)</sup>. The meaning of the new fundamental densities was explained more clearly by introducing auxiliary functions derived from original unknown functions<sup>(36)</sup>. In this paper, numerical solutions will be shown precisely but concisely because they are essentially based on the previous studies<sup>(34)–(36)</sup>.

First, several important notations are shown to describe the numerical solutions for Fig. 1 (a).

$(r, \theta, z)$  : a point in a cylindrical coordinate in Fig. 1

$(\rho, \varphi, \zeta)$  : a point where body forces are applied

$\psi, \alpha$  : parametric angle of ellipsoid

$(\rho = a \cos \alpha_j, \zeta = d + b \sin \alpha_j, (j = 1, 2)$  and,  $r = a \cos \psi_i, z = d + b \sin \psi_i, (i = 1, 2)$ )

$\psi_{i0}$  : Angle between the  $r$ -axis and the normal direction of ellipsoid at  $(r, z)$ ;  $\tan \psi_{i0} = (a/b) \tan \psi_i, (i = 1, 2)$

$F_{rj}, F_{zj}$  : ring forces in the  $r$ - and  $z$ -directions at  $(\rho, \varphi, \zeta)$

$\sigma_r^{Frj}$  : normal stress in the  $r$ -direction due to a ring force

$$K_{nm}^{Frj} : K_{nm}^{Frj} = \sigma_n^{Frj} = \sigma_r^{Frj} \cos^2 \psi_{i0} + \sigma_z^{Frj} \sin^2 \psi_{i0} + 2\tau_{rz}^{Frj} \cos \psi_{i0} \sin \psi_{i0}$$

$\rho_{rMj}^*(\alpha_j)$  : body force densities distributed in the bodies  $M_j$  in the  $r$ -direction

The body force method is used to formulate the problem as a system of singular integral equations. The method requires fundamental solutions, that is, the stress  $(K_{nm}^{Frj}, K_{nm}^{Fzj}, K_{nt}^{Frj}, K_{nt}^{Fzj})$  and displacement fields  $(K_{ur}^{Fr}, K_{ur}^{Fz}, K_{uz}^{Fr}, K_{uz}^{Fz})$  at an arbitrary point  $(r, \theta, z)$  when ring forces are

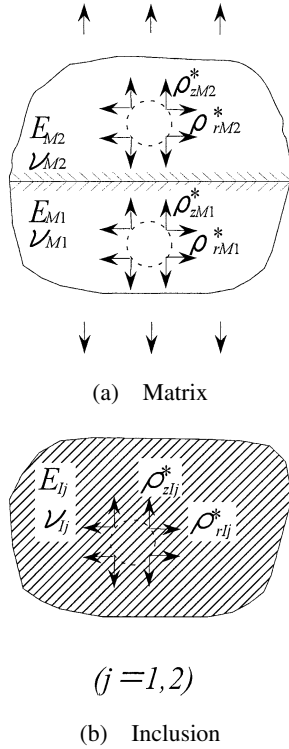


Fig. 2 Method of solution

acting in the  $r$ - and  $z$ -directions at  $(\rho, \varphi, \zeta)$  in a bimaterial body. Here,  $(\rho, \varphi, \zeta)$  is a point in the  $(r, \theta, z)$  coordinate system where ring forces are applied. For example, in the analysis of Fig. 1 (a), we can express that  $\rho = a \cos \alpha$ ,  $\zeta = d + b \sin \alpha$ , and  $r = a \cos \psi$ ,  $z = d + b \sin \psi$ .

In the analysis of Fig. 1 (c), a bimaterial body “ $M_j$ ” and two infinite body “ $I_j$ ” are considered, each of which having the same elastic constants as those of the matrix  $(E_{M_j}, \nu_{M_j})$  and inclusion  $(E_{I_j}, \nu_{I_j})$  as shown in Fig. 2. Denote  $\sigma_{nM}$ ,  $\tau_{ntM}$ ,  $u_{rM}$ ,  $u_{zM}$  as stresses and displacements which appear along the prospective elliptical boundaries which appear along the prospective elliptical boundaries in the bimaterial body “ $M_j$ ”. In a similar way, denote  $\sigma_{nI}$ ,  $\tau_{ntI}$ ,  $u_{rI}$ ,  $u_{zI}$  as stresses and displacements which appear along the prospective elliptical boundaries in the infinite body “ $I_j$ ”. Then, a boundary condition for inclusion  $i$ , for example,  $\sigma_{nM} - \sigma_{nI} = 0$ , can be expressed as Eq. (1).

$$\begin{aligned}
 & -\frac{1}{2} \left\{ \rho_{rMi}^*(\psi_i) \cos \psi_{i0} + \rho_{zMi}^*(\psi_i) \sin \psi_{i0} \right\} \\
 & -\frac{1}{2} \left\{ \rho_{rIi}^*(\psi_i) \cos \psi_{i0} + \rho_{zIi}^*(\psi_i) \sin \psi_{i0} \right\} \\
 & + \sum_{j=1}^2 \left[ \int_{-\pi/2}^{\pi/2} K_{nmMi}^{Frj}(\alpha_j, \psi_i) \rho_{rMj}^*(\alpha_j) ds \right. \\
 & + \int_{-\pi/2}^{\pi/2} K_{nmMi}^{Fzj}(\alpha_j, \psi_i) \rho_{zMj}^*(\alpha_j) ds \\
 & - \int_{-\pi/2}^{\pi/2} K_{nnIi}^{Frj}(\alpha_j, \psi_i) \rho_{rIj}^*(\alpha_j) ds \\
 & \left. - \int_{-\pi/2}^{\pi/2} K_{nnIi}^{Fzj}(\alpha_j, \psi_i) \rho_{zIj}^*(\alpha_j) ds \right]
 \end{aligned}$$

$$= -(\sigma_z^\infty \sin^2 \psi_{i0} + \sigma_{rI}^\infty \cos^2 \psi_{i0}) \quad (i = 1, 2) \quad (1)$$

where

$$\begin{cases}
 -\frac{\pi}{2} \leq \psi_j \leq \frac{\pi}{2}, \\
 -d\rho = a_j \sin \alpha_j d\alpha_j, \\
 d\zeta = b_j \cos \alpha_j d\alpha_j, \\
 ds = \sqrt{a_j^2 \sin^2 \alpha_j + b_j^2 \cos^2 \alpha_j} d\alpha_j,
 \end{cases} \quad (j = 1, 2) \quad (2)$$

In Eq. (1), unknowns are the body force densities  $\rho_{rM_j}^*(\alpha_j)$ ,  $\rho_{zM_j}^*(\alpha_j)$ ,  $\rho_{rI_j}^*(\alpha_j)$ ,  $\rho_{zI_j}^*(\alpha_j)$  distributed in the bodies  $M_j$  and  $I_j$  in the  $r$ - and  $z$ -directions along the circumference, which is specified by the angle  $\alpha_j$ . Other boundary conditions,  $\tau_{ntM} - \tau_{ntI} = 0$ ,  $u_{rM} - u_{rI} = 0$ ,  $u_{zM} - u_{zI} = 0$ , are given in a similar way. Here  $\psi_{i0}$  is the angle between the  $r$ -axis and the normal direction of an ellipsoidal inclusion at  $(r, z)$ . Equation (1) includes Cauchy-type singular terms; therefore, the integral in Eq. (1) should be taken in a sense of Cauchy’s of principal value when  $\psi_i = \alpha_j$  ( $i = j$ ). The first and second terms of Eq. (1) represent the stress due to the body force distributed on the imaginary boundary, which is composed of the internal or external points that are infinitesimally apart from the initial boundary<sup>(33)</sup>. Taking  $K_{nmMi}^{Frj}(\alpha_j, \psi_i)$  for example, the notation means the normal stress  $\sigma_{nMi}$  induced at the point when a ring force  $F_{rj}$  in the  $r$ -direction is acting on the imaginary boundary in bimaterial body “ $M_1$ ” or “ $M_2$ ”. These expressions can be derived by integrating the fundamental solution due to a point force<sup>(37)</sup> in the  $\theta$ -direction. The fundamental stress and displacement fields due to a ring force in a bimaterial body are shown in the appendix.

In the present analysis, the unknown body force densities are approximated as a linear combination of fundamental density functions and weight functions as shown in the Eq. (3) (see Refs. (34)–(36)).

$$\begin{cases}
 \rho_{rM_j}^*(\alpha_j) = \rho_{r3M_j}(\alpha_j) w_{r3}(\alpha_j) + \rho_{r4M_j}(\alpha_j) w_{r4}(\alpha_j), \\
 \rho_{zM_j}^*(\alpha_j) = \rho_{z1M_j}(\alpha_j) w_{z1}(\alpha_j) + \rho_{z2M_j}(\alpha_j) w_{z2}(\alpha_j), \\
 \rho_{rI_j}^*(\alpha_j) = \rho_{r3I_j}(\alpha_j) w_{r3}(\alpha_j) + \rho_{r4I_j}(\alpha_j) w_{r4}(\alpha_j), \\
 \rho_{zI_j}^*(\alpha_j) = \rho_{z1I_j}(\alpha_j) w_{z1}(\alpha_j) + \rho_{z2I_j}(\alpha_j) w_{z2}(\alpha_j).
 \end{cases} \quad (j = 1, 2) \quad (3)$$

Here, the fundamental density functions<sup>(34)–(36)</sup> are defined by Eqs. (4) and (5). In these equations,  $w_{r3}(\alpha)$ ,  $w_{z2}(\alpha)$  are exact densities to express the stress field due to an ellipsoidal inclusion in an infinite body.

$$\begin{cases}
 w_{r3}(\alpha) = n_r(\alpha), & w_{r4}(\alpha) = n_r(\alpha) \sin \alpha, \\
 w_{z1}(\alpha) = n_z(\alpha) / \sin \alpha, & w_{z2}(\alpha) = n_z(\alpha).
 \end{cases} \quad (4)$$

$$\begin{cases}
 n_r(\alpha) = \frac{b \cos \alpha}{\sqrt{a^2 \sin^2 \alpha + b^2 \cos^2 \alpha}}, \\
 n_z(\alpha) = \frac{a \sin \alpha}{\sqrt{a^2 \sin^2 \alpha + b^2 \cos^2 \alpha}}.
 \end{cases} \quad (5)$$

On the other hand, the weight functions are approximated by using polynomials as shown in Eq. (6).

$$\left\{ \begin{aligned} \rho_{r3M_j}(\alpha_j) &= \sum_{n=1}^{M/2} a_{nM_j} t_n(\alpha_j), & \rho_{r3I_j}(\alpha_j) &= \sum_{n=1}^{M/2} a_{nI_j} t_n(\alpha_j), \\ \rho_{r4M_j}(\alpha_j) &= \sum_{n=1}^{M/2} b_{nM_j} t_n(\alpha_j), & \rho_{r4I_j}(\alpha_j) &= \sum_{n=1}^{M/2} b_{nI_j} t_n(\alpha_j), \\ \rho_{z1M_j}(\alpha_j) &= \sum_{n=1}^{M/2} c_{nM_j} t_n(\alpha_j), & \rho_{z1I_j}(\alpha_j) &= \sum_{n=1}^{M/2} c_{nI_j} t_n(\alpha_j), \\ \rho_{z2M_j}(\alpha_j) &= \sum_{n=1}^{M/2} d_{nM_j} t_n(\alpha_j), & \rho_{z2I_j}(\alpha_j) &= \sum_{n=1}^{M/2} d_{nI_j} t_n(\alpha_j). \end{aligned} \right. \quad (i = 1, 2) \quad (6)$$

$$t_n(\alpha_j) = \cos\{2(n-1)\alpha_j\}$$

where  $M$  is the number of the collocation points in the range  $-\pi/2 \leq \alpha_j \leq \pi/2$ . Using the approximation method mentioned above, we obtain a system of linear equations for the determination of the coefficients  $a_{nM_j} \sim d_{nI_j}$ . The number of unknown coefficients is  $4M \times 2$ . The collocation points are set as given by Eq. (7).

$$\theta_L = \frac{\pi}{M}(L-0.5) - \frac{\pi}{2} \quad L = 2, 3, \dots, M. \quad (7)$$

Using the numerical solution mentioned above we will obtain the stress distribution along the interface and discuss the maximum stress.

#### 4. Results and Discussion

##### 4.1 Convergence of the results

First, in Fig. 1 (b), we put  $\sigma_{r1}^\infty = \sigma_{\theta1}^\infty = 1$ ,  $\sigma_z^\infty = 0$ ,  $a/b = 1$ ,  $b/d = 0.9$ ,  $E_1/E_{M1} = 0$ ,  $E_{M2}/E_{M1} = 0$ , and Poisson's ratio  $\nu_{M1} = 0.3$ . Then, Table 1 shows the convergence of interface stresses  $\sigma_{tM}$ ,  $\sigma_{nM}$ ,  $\sigma_{ntM}$ ,  $\sigma_{tl}$ ,  $\sigma_{nl}$ ,  $\sigma_{ntl}$  at A in Fig. 1 (b) with increasing the collocation number  $M$  for two spheroidal cavities in a semi-infinite body. The present results show good convergence to the sixth digit even for the case of  $b/d = 0.9$ .

##### 4.2 Results of an ellipsoidal inclusion in the vicinity of an interface

Figure 3 shows an example of the results of an ellipsoidal inclusion near an interface. More detail results may be found in Refs. (38)–(41). In this paper, the results of two spheroidal inclusions will be mainly shown.

Table 1 Convergence of interface stresses at A when  $a/b = 1$ ,  $b/d = 0.9$ ,  $E_1/E_{M1} = 0$ ,  $E_{M2}/E_{M1} = 0$ ,  $\sigma_{r1}^\infty = \sigma_{\theta1}^\infty = 1$ ,  $\sigma_z^\infty = 0$  in Fig. 1 (b)

M	$\sigma_{tM}$	$\sigma_{tl}$	$\sigma_{nM}$	$\sigma_{nl}$	$\sigma_{ntM}$	$\sigma_{ntl}$
24	2.80738	$3.0 \times 10^{-6}$	$-7.0 \times 10^{-6}$	$5.3 \times 10^{-6}$	$-3.1 \times 10^{-6}$	$2.5 \times 10^{-8}$
36	2.80737	$3.0 \times 10^{-6}$	$4.5 \times 10^{-7}$	$5.3 \times 10^{-6}$	$-1.1 \times 10^{-6}$	$2.5 \times 10^{-8}$
48	2.80737	$3.0 \times 10^{-6}$	$4.9 \times 10^{-7}$	$5.3 \times 10^{-6}$	$-4.5 \times 10^{-7}$	$2.5 \times 10^{-8}$

##### 4.3 Results of two spheroidal cavities in an infinite body

Table 2 shows the maximum stress and the stress at the point  $\psi = 0^\circ$  for the problem of two spheroidal cavities in an infinite body with the results of Nisitani's approximate calculation<sup>(7)</sup> and Miyamoto's solution<sup>(11)</sup>. In the analysis, the Green's function for a ring force in an infinite body was used<sup>(42)</sup>. The angle  $\psi$  in Table 2 shows the position of maximum stress. It is seen that Nisitani's results, which are based on a simple calculation, are more accurate than Miyamoto's results, which are based on a complicated three-dimensional theory of elasticity.

##### 4.4 Results of two spheroidal inclusions in the vicinity of an interface

Table 3 and Fig. 4 show the results of two spheroidal cavities in a semi-infinite body under biaxial tension. Here, the stresses  $\sigma_t = \sigma_\theta$  at A ( $\psi_1 = -90^\circ$ ), B ( $\psi_1 = 90^\circ$ ), C ( $\psi_2 = -90^\circ$ ), D ( $\psi_2 = 90^\circ$ ) are indicated. It is seen that the stress at A rapidly increases as  $b/d \rightarrow 1$ . On the other hand, the stresses at B and C decreases in the range  $b/d = 0.4 - 0.8$  and finally increases when  $b/d = 0.85 - 1$ . The stress at D is almost constant independent of the size of the cavities.

Figure 5 (a) shows the results of two spheroidal cavities near an interface under longitudinal tension. With increasing elastic modulus ratio of the matrix  $E_{M2}/E_{M1}$ ,

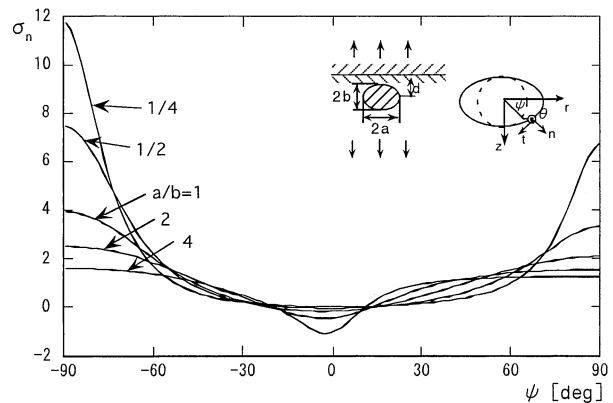


Fig. 3 Interface stress  $\sigma_n$  when  $\sigma_z^\infty = 1$ ,  $\sigma_{r1}^\infty = \sigma_{\theta1}^\infty = \sigma_{r2}^\infty = \sigma_{\theta2}^\infty = 0$ ,  $\nu_{M1} = \nu_{I1} = 0.3$ ,  $E_1/E_{M1} = E_{M2}/E_{M1} = \infty$  in Fig. 1 (a)

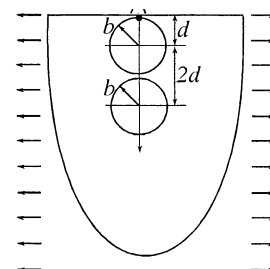


Table 2 Maximum stress  $\sigma_t$  at A and B for two spheroidal cavities in an infinite body when  $a_1/b_1 = a_2/b_2 = 1$ ,  $\nu_{M1} = \nu_{M2} = 0.3$ ,  $E_{M1} = E_{M2} = E_M$ ,  $E_{I1}/E_M = E_{I2}/E_M = 0$ ,  $\sigma_{r1}^\infty = \sigma_{r2}^\infty = \sigma_{\theta2}^\infty = 0$ ,  $\sigma_z^\infty = 1$  in Fig. 1 (c).

b/d	0	0.1	0.2	0.3	0.4	0.5	0.6	0.7	0.8	0.9
$\sigma_t$ at A	2.0217	2.0209	2.0157	2.0031	1.9830	1.9584	1.9338	1.9124	1.8951	1.8810
( $\psi$ )	(0°)	(0°)	(0°)	(0.2°)	(0.5°)	(1.0°)	(2.0°)	(2.7°)	(3.4°)	(3.8°)
at B	2.0217	2.0209	2.0157	2.0031	1.9828	1.9573	1.9306	1.9062	1.8854	1.8676
Nisitani [7]	2.022	2.021	2.016	2.003	1.983	1.959	(1.941)	(1.944)	(1.994)	(2.147)
Miyamoto [11]	2.022	2.021	2.016	2.002	1.986	1.969				

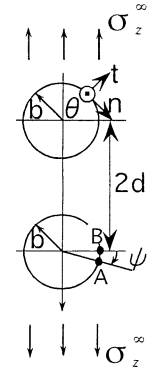


Table 3 Interface stress  $\sigma_t = \sigma_\theta$  at points A, B, C, D of two spheroidal cavities in a semi-infinite body when  $a_1/b_1 = a_2/b_2 = 1$ ,  $\nu_{M1} = 0.3$ ,  $E_{M2}/E_{M1} = 0$ ,  $E_{I1}/E_{M1} = 0$ ,  $\sigma_{r1}^\infty = \sigma_{\theta1}^\infty = 1$ ,  $\sigma_z^\infty = 0$  in Fig. 1 (b)

b/d	0	0.2	0.4	0.6	0.7	0.8	0.9
$\sigma_t = \sigma_\theta$ at A	2.1820	2.1867	2.2400	2.3940	2.4859	2.5582	2.8074
B	2.1820	2.1818	2.1657	2.0864	2.0400	2.1068	2.6628
C	2.1820	2.1798	2.1550	2.0578	2.0043	2.0731	2.6416
D	2.1820	2.1811	2.1787	2.1744	2.1731	2.1739	2.1783

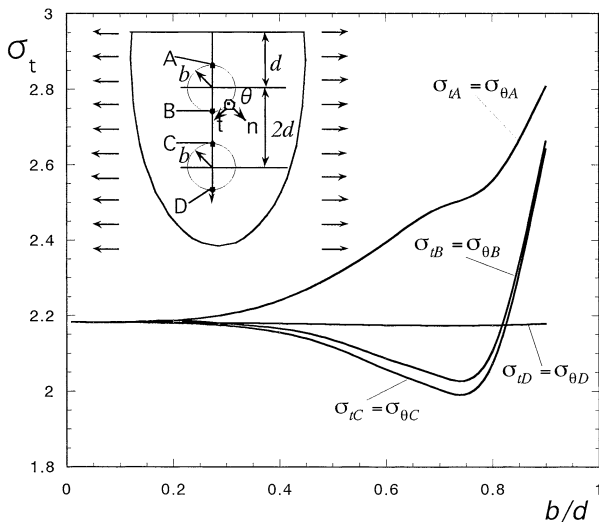
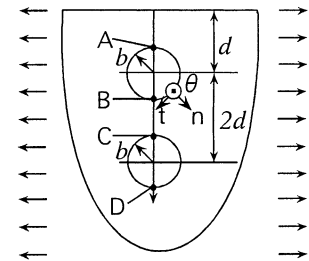


Fig. 4 Interface stress  $\sigma_t = \sigma_\theta$  at points A, B, C, D for two spheroidal cavities when  $E_{M2}/E_{M1} = 0$ ,  $E_{I1}/E_{M1} = 0$ ,  $a_1/b_1 = a_2/b_2 = 1$ ,  $\nu_{M1} = 0.3$ ,  $\sigma_{r1}^\infty = \sigma_{\theta1}^\infty = 1$ ,  $\sigma_z^\infty = 0$  in Fig. 1 (b)

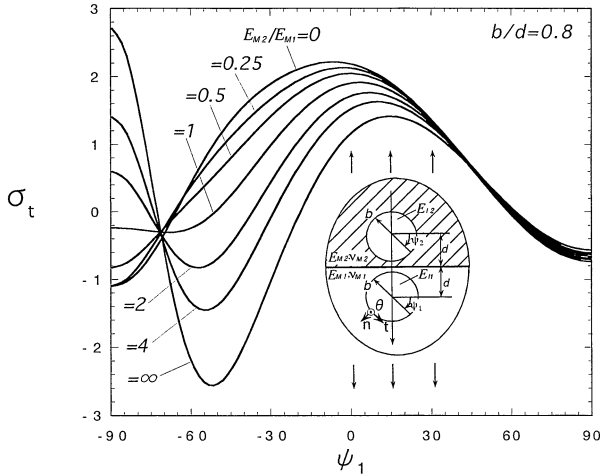
the position of the maximum stress varies from  $\psi_1 \cong 0^\circ$  to  $\psi_1 = 90^\circ$ . Also, Fig. 5 (b) shows the results of two spheroidal rigid inclusions near an interface. With increasing elastic modulus ratio of the matrix  $E_{M2}/E_{M1}$ , the maximum stress  $\sigma_n$  increases at  $\psi_1 = -90^\circ$ .

### 5. Conclusion

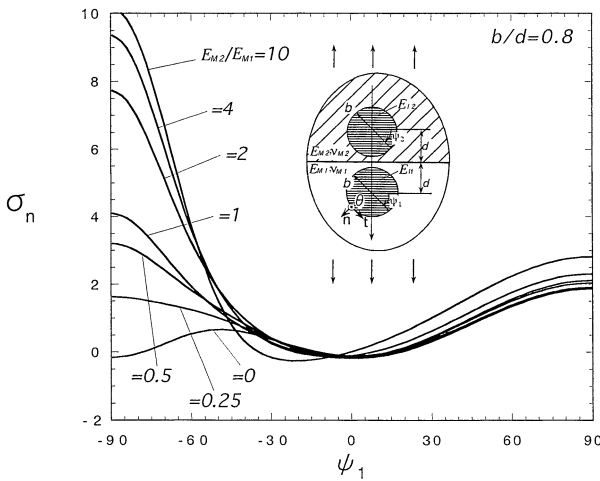
In this study, ellipsoidal inclusions of revolution in the vicinity of a bimaterial interface were considered by using the body force method. First, all components of stress and displacement were shown when ring forces are acting in the  $r$ - and  $z$ -directions in a three-dimensional bimaterial body (see Fig. 6). Then, the problems were solved using the body force method coupled with a system of singular integral formulation. In order to satisfy the boundary conditions, the unknown functions were approximated by a linear combination of fundamental density functions and polynomials. The preset method was found to yield rapidly converging numerical results and smooth stress distribution along the boundary. Several interaction problems among the inclusions and interface were discussed with varying the aspect ratio, elastic modulus ratio, and spacing of inclusions.

### Appendix: Stress and displacement due to a ring force in a bimaterial body

In the following Eqs.,  $(r, \theta, z)$  is a point in question, and  $(\rho, \varphi, \zeta)$  is a point where ring forces are applied. Then, as shown in Fig. 6 (a), the stress and displacement fields in material 2 when ring forces are applied in the  $r$ - and  $z$ -directions in material 1 can be expressed as shown in Eqs. (8)–(21).



(a) Interface stress  $\sigma_t$  when  $E_{I1}/E_{M1} = E_{I2}/E_{M1} = 0$

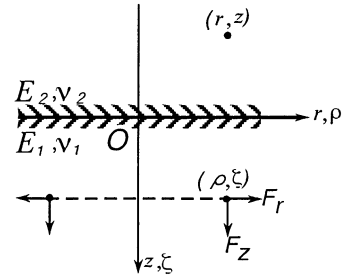


(b) Interface stress  $\sigma_n$  when  $E_{I1}/E_{M1} = E_{I2}/E_{M1} = \infty$

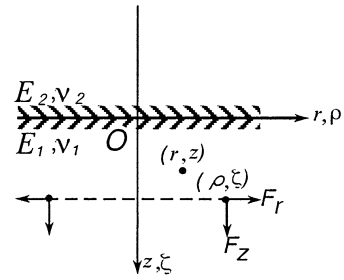
Fig. 5 Interface stress when  $a_1/b_1 = a_2/b_2 = 1$ ,  $\sigma_{r1}^\infty = \sigma_{\theta 1}^\infty = \sigma_{r2}^\infty = \sigma_{\theta 2}^\infty = 0$ ,  $\nu_{M1} = \nu_{M2} = \nu_{I1} = \nu_{I2} = 0.3$ , in Fig. 1 (c)

$$\left\{ \begin{aligned} K_{mnM_i}^{Frj} &= \sigma_n^{Fr} \\ &= \sigma_r^{Fr} \cos^2 \psi_{i0} + \sigma_z^{Fr} \sin^2 \psi_{i0} + 2\tau_{rz}^{Fr} \cos \psi_{i0} \sin \psi_{i0}, \\ K_{mnM_i}^{Fzj} &= \sigma_n^{Fz} \\ &= \sigma_r^{Fz} \cos^2 \psi_{i0} + \sigma_z^{Fz} \sin^2 \psi_{i0} + 2\tau_{rz}^{Fz} \cos \psi_{i0} \sin \psi_{i0}, \\ K_{ntM_i}^{Frj} &= \tau_{nt}^{Fr} = (\sigma_z^{Fr} - \sigma_r^{Fr}) \cos \psi_{i0} \sin \psi_{i0} \\ &\quad + \tau_{rz}^{Fr} (\cos^2 \psi_{i0} - \sin^2 \psi_{i0}), \\ K_{ntM_i}^{Fzj} &= \tau_{nt}^{Fz} = (\sigma_z^{Fz} - \sigma_r^{Fz}) \cos \psi_{i0} \sin \psi_{i0} \\ &\quad + \tau_{rz}^{Fz} (\cos^2 \psi_{i0} - \sin^2 \psi_{i0}). \end{aligned} \right. \quad (i = 1, 2) \quad (8)$$

$$\begin{aligned} K_{ur}^{Fr} &= U_r^{Fr} \\ &= C \left\{ \frac{1}{2} \left[ 2\kappa_1(1-\bar{A}) - ES(\kappa_1-1)(\kappa_2+1) \right] r_m^2 I_{1,1} \right. \\ &\quad \left. - (1-\bar{A}) \left\{ r\rho I_{3,0} - (r^2 + \rho^2) I_{3,1} + r\rho I_{3,2} \right\} \right\} \end{aligned}$$



(a) Stress and displacement in material 2 due to a ring force in the  $r$ - or  $z$ -direction in material 1



(b) Stress and displacement in material 1 due to a ring force in the  $r$ - or  $z$ -direction in material 1

Fig. 6 Ring forces acting in the  $r$ - and  $z$ -directions in a bimaterial

$$\begin{aligned} &+ \int_0^\pi \left\{ -\bar{T}S(\kappa_2+1)z \left[ \frac{\cos \varphi}{R_1(R_1-z+\zeta)} \right. \right. \\ &+ \left. \left. \frac{2R_1-z+\zeta}{R_1^3(R_1-z+\zeta)^2} \left\{ r\rho - (r^2 + \rho^2) \cos \varphi + r\rho \cos^2 \varphi \right\} \right] \right. \\ &+ \left. \frac{1}{2}S(\kappa_2+1)[E(\kappa_1-1)-2T] \right. \\ &\times \left. \left[ \frac{\cos \varphi}{R_1-z+\zeta} + \frac{1}{R_1(R_1-z+\zeta)^2} \right. \right. \\ &\times \left. \left. \left\{ r\rho - (r^2 + \rho^2) \cos \varphi + r\rho \cos^2 \varphi \right\} \right] \right\} d\varphi \quad (9) \end{aligned}$$

$$\begin{aligned} K_{uz}^{Fr} &= U_z^{Fr} \\ &= C \left\{ [(1-\bar{A})(z-\zeta) - \bar{T}S(\kappa_2+1)z] (-\rho I_{3,0} + rI_{3,1}) \right. \\ &+ \left. C \int_0^\pi \left\{ \frac{TS(\kappa_2+1)}{R_1(R_1-z+\zeta)} (-\rho + r \cos \varphi) \right\} d\varphi \right\} \quad (10) \end{aligned}$$

$$\begin{aligned} K_{ur}^{Fz} &= U_r^{Fz} \\ &= C \left\{ [(1-\bar{A})(z-\zeta) - \bar{T}S(\kappa_2+1)z] (rI_{3,0} - \rho I_{3,1}) \right. \\ &- \left. C \int_0^\pi \left\{ \frac{TS(\kappa_2+1)}{R_1(R_1-z+\zeta)} (r - \rho \cos \varphi) \right\} d\varphi \right\} \quad (11) \end{aligned}$$

$$\begin{aligned} K_{uz}^{Fz} &= U_z^{Fz} \\ &= C \left\{ [(1-\bar{A})\kappa_1 - TS(\kappa_2+1)] r_m^2 I_{1,0} \right. \\ &+ \left. [(1-\bar{A})(z-\zeta)^2 - \bar{T}S(\kappa_2+1)z(z-\zeta)] I_{3,0} \right\} \quad (12) \end{aligned}$$

$$\sigma_r^{Fr} = D \left\{ \frac{1}{2} \left\{ (\kappa_2-3)(1-\bar{B}) + 2(1-\bar{A}) \right\} (-\rho I_{3,0} + rI_{3,1}) \right.$$

$$\begin{aligned}
 & + \frac{1}{2} [2(1-\bar{A}) - ES(\kappa_2 + 1)](1 - \kappa_1)(rI_{3,1} - \rho I_{3,2}) \\
 & - 3(1-\bar{A}) \left\{ -r^2 \rho I_{5,0} + r(r^2 + 2\rho^2)I_{5,1} \right. \\
 & \left. - \rho(\rho^2 + 2r^2)I_{5,2} + r\rho^2 I_{5,3} \right\} / r_m^2 \\
 & + \int_0^\pi \left[ \frac{1}{2} S(\kappa_2 + 1)[2T - E(\kappa_1 - 1)] \right. \\
 & \times \left[ \frac{-\rho + 3r \cos \varphi - 2\rho \cos^2 \varphi}{R_1(R_1 - z + \zeta)^2} \right. \\
 & \left. - \frac{3R_1 - z + \zeta}{R_1(R_1 - z + \zeta)^3} \left\{ -r^2 \rho + r(r^2 + 2\rho^2) \cos \varphi \right. \right. \\
 & \left. \left. - \rho(\rho^2 + 2r^2) \cos^2 \varphi + r\rho^2 \cos^3 \varphi \right\} \right] \\
 & + \bar{T}S(\kappa_2 + 1)z \\
 & \times \left[ \frac{2R_1 - z + \zeta}{R_1^3(R_1 - z + \zeta)^2} (-\rho + 3r \cos \varphi - 2\rho \cos^2 \varphi) \right. \\
 & \left. - \left\{ \frac{3(2R_1 - z + \zeta)}{R_1^5(R_1 - z + \zeta)^2} + \frac{2}{R_1^3(R_1 - z + \zeta)^3} \right\} \right. \\
 & \left. \times \left\{ -r^2 \rho + r(r^2 + 2\rho^2) \cos \varphi \right. \right. \\
 & \left. \left. - \rho(\rho^2 + 2r^2) \cos^2 \varphi + r\rho^2 \cos^3 \varphi \right\} \right] d\varphi \Big\} \quad (13)
 \end{aligned}$$

$$\begin{aligned}
 \sigma_z^{Fr} = D \Big\{ & \frac{1}{2} \left\{ (\kappa_2 - 3)(1 - \bar{B}) + 2(1 - \bar{A}) \right. \\
 & + 2(T - \bar{T})S(\kappa_2 + 1) \left. \right\} (-\rho I_{3,0} + rI_{3,1}) \\
 & + \left[ 3\bar{T}S(\kappa_2 + 1)z(z - \zeta) - 3(1 - \bar{A})(z - \zeta)^2 \right] \\
 & \left. \times (-\rho I_{5,0} + rI_{5,1}) / r_m^2 \right\} \quad (14)
 \end{aligned}$$

$$\begin{aligned}
 \sigma_\theta^{Fr} = D \Big\{ & \frac{1}{2} \left\{ (\kappa_2 - 3)(1 - \bar{B}) + 2(1 - \bar{A}) \right\} (-\rho I_{3,0} + rI_{3,1}) \\
 & + \frac{1}{2} [2(1 - \bar{A}) - ES(\kappa_2 + 1)](1 - \kappa_1)\rho(-I_{3,0} + I_{3,2}) \\
 & + 3(1 - \bar{A})\rho^2(\rho I_{5,0} - rI_{5,1} - \rho I_{5,2} + rI_{5,3}) / r_m^2 \Big\} \\
 & + D \int_0^\pi \left[ -\frac{1}{2} S(\kappa_2 + 1)[E(\kappa_1 - 1) - 2T] \right. \\
 & \times \left[ \frac{-3\rho + r \cos \varphi + 2\rho \cos^2 \varphi}{R_1(R_1 - z + \zeta)^2} \right. \\
 & \left. + \frac{3R_1 - z + \zeta}{R_1^3(R_1 - z + \zeta)^3} \rho^2(\rho - r \cos \varphi - \rho \cos^2 \varphi + r \cos^3 \varphi) \right] \\
 & - \bar{T}S(\kappa_2 + 1)z \\
 & \times \left[ \frac{2R_1 - z + \zeta}{R_1^3(R_1 - z + \zeta)^2} (3\rho - r \cos \varphi - 2\rho \cos^2 \varphi) \right. \\
 & \left. - \left\{ \frac{3(2R_1 - z + \zeta)}{R_1^5(R_1 - z + \zeta)^2} + \frac{2}{R_1^3(R_1 - z + \zeta)^3} \right\} \right. \\
 & \left. \times \rho^2(\rho - r \cos \varphi - \rho \cos^2 \varphi + r \cos^3 \varphi) \right] d\varphi \Big\} \quad (15)
 \end{aligned}$$

$$\times \rho^2(\rho - r \cos \varphi - \rho \cos^2 \varphi + r \cos^3 \varphi) \Big\} d\varphi \quad (15)$$

$$\begin{aligned}
 \tau_{rz}^{Fr} = D \Big\{ & \frac{1}{4} \left\{ [2(1 - \kappa_1)(1 - \bar{A}) + ES(\kappa_1 - 1)](z - \zeta) \right. \\
 & \left. - 4\bar{T}S(\kappa_2 + 1)z \right\} I_{3,1-3} \left[ (1 - \bar{A})(z - \zeta) - \bar{T}S(\kappa_2 + 1)z \right] \\
 & \times \left\{ -r\rho I_{5,0} + (r^2 + \rho^2)I_{5,1} - r\rho I_{5,2} \right\} / r_m^2 \Big\} \\
 & - D \int_0^\pi \left\{ \frac{S(\kappa_2 + 1)[E(\kappa_1 - 1) - 2\bar{T}](2R_1 - z + \zeta)}{4R_1^3(R_1 - z + \zeta)^2} \right. \\
 & \times \left\{ -r\rho + (r^2 + \rho^2) \cos \varphi - r\rho \cos^2 \varphi \right\} \\
 & \left. - \frac{S(\kappa_2 + 1)[E(\kappa_1 - 1) - 2\bar{T}]}{4R_1(R_1 - z + \zeta)} \cos \varphi \right\} d\varphi \quad (16)
 \end{aligned}$$

$$\begin{aligned}
 \sigma_r^{Fz} = D \Big\{ & \frac{1}{2} \left\{ [(\kappa_2 - 3)(1 - \bar{B}) + 2(1 - \bar{A})](z - \zeta) \right. \\
 & \left. - 2\bar{T}S(\kappa_2 + 1)z \right\} I_{3,0} \\
 & + 3 \left[ \bar{T}S(\kappa_2 + 1)z - (1 - \bar{A})(z - \zeta) \right] \\
 & \times (r^2 I_{5,0} - 2r\rho I_{5,1} + \rho^2 I_{5,2}) / r_m^2 \Big\} \\
 & - D \int_0^\pi \left\{ \frac{TS(\kappa_2 + 1)}{R_1(R_1 - z + \zeta)} - \frac{TS(\kappa_2 + 1)(2R_1 - z + \zeta)}{R_1^3(R_1 - z + \zeta)^2} \right. \\
 & \left. \times (r^2 - 2r\rho \cos \varphi + \rho^2 \cos^2 \varphi) \right\} d\varphi \quad (17)
 \end{aligned}$$

$$\begin{aligned}
 \sigma_z^{Fz} = D \Big\{ & \frac{1}{2} \left\{ [(\kappa_2 - 3)(1 - \bar{B}) + 2(2 - \kappa_1)(1 - \bar{A}) \right. \\
 & + 2(T - \bar{T})S(\kappa_2 + 1)](z - \zeta) - 2\bar{T}S(\kappa_2 + 1)z \Big\} I_{3,0} \\
 & + 3(z - \zeta)^2 \left[ \bar{T}S(\kappa_2 + 1)z - (1 - \bar{A})(z - \zeta) \right] I_{5,0} / r_m^2 \Big\} \quad (18)
 \end{aligned}$$

$$\begin{aligned}
 \sigma_\theta^{Fz} = D \Big\{ & \frac{1}{2} \left\{ [(\kappa_2 - 3)(1 - \bar{B}) + 2(1 - \bar{A})](z - \zeta) \right. \\
 & \left. - 2\bar{T}S(\kappa_2 + 1)z \right\} I_{3,0} \\
 & + 3 \left[ \bar{T}S(\kappa_2 + 1)z - (1 - \bar{A})(z - \zeta) \right] \rho^2(I_{5,0} - I_{5,2}) / r_m^2 \Big\} \\
 & - D \int_0^\pi \left\{ \left[ \frac{TS(\kappa_2 + 1)}{R_1(R_1 - z + \zeta)} - \frac{TS(\kappa_2 + 1)(2R_1 - z + \zeta)}{R_1^3(R_1 - z + \zeta)^2} \right] \right. \\
 & \left. \times \rho^2(1 - \cos^2 \varphi) \right\} d\varphi \quad (19)
 \end{aligned}$$

$$\begin{aligned}
 \tau_{rz}^{Fz} = D \Big\{ & -\frac{1}{2} \left\{ \bar{T}S(\kappa_2 + 1) + (\kappa_1 - 1)(1 - \bar{A}) \right\} (rI_{3,0} - \rho I_{3,1}) \\
 & + 3 \left[ \bar{T}S(\kappa_2 + 1)z(z - \zeta) + (\bar{A} - 1)(z - \zeta)^2 \right] \\
 & \left. \times (rI_{5,0} - \rho I_{5,1}) / r_m^2 \right\} \quad (20)
 \end{aligned}$$

where

$$\left\{ \begin{array}{l}
 I_{n,m} = \int_0^\pi \frac{\cos^m \varphi}{(e_1 - \cos \varphi)^{n/2}} d\varphi, \\
 e_1 = 1 + \frac{(r-\rho)^2 + (z+\zeta)^2}{2r\rho}, \\
 \kappa_1 = 3 - 4\nu_{M1}, \quad \kappa_2 = 3 - 4\nu_{M2}, \quad \Gamma = \frac{G_{M2}}{G_{M1}}, \\
 S = \frac{2}{1+\Gamma}, \quad \bar{A} = \frac{\Gamma\kappa_1 - \kappa_2}{1 + \Gamma\kappa_1}, \quad \bar{B} = \frac{\Gamma - 1}{\kappa_2 + \Gamma}, \\
 C = \frac{\Gamma\rho}{2\mu_2\pi(\kappa_2 + 1)r_m^3}, \quad D = \frac{\Gamma\rho}{\pi(\kappa_2 + 1)r_m^3}, \\
 E = \frac{1 - \Gamma}{1 + \Gamma\kappa_1}, \\
 T = \frac{1}{4} \left[ \frac{\kappa_1 - 1}{1 + \Gamma\kappa_1} - \frac{(\kappa_2 - 1)\Gamma}{\kappa_2 + \Gamma} \right], \\
 \bar{T} = \frac{1}{2} \left[ \frac{\kappa_2 - 1}{\kappa_2 + \Gamma} - \frac{(\kappa_1 - 1)\Gamma}{1 + \Gamma\kappa_1} \right], \\
 r_m = \sqrt{2r\rho}, \quad R_1^2 = r^2 + \rho^2 + (z - \zeta)^2 - 2r\rho\cos\varphi
 \end{array} \right. \quad (21)$$

Here,  $I_{n,m}$  ( $n = 3, 5, 7, m = 0, 1, 2, 3$ ) can be expressed by using complete elliptic integrals<sup>(42), (43)</sup>. Also,  $G_{M1}, G_{M2}$  are moduli of transverse elasticity of each material.

Similarly, the stress and displacement fields in material 1 when ring forces are applied in the  $r$ - and  $z$ -directions in material 1 have been given as Eqs. (14)–(28) in Ref. (39). Furthermore, Hasegawa et al. have derived equivalent fundamental Green's functions due to ring forces in a biomaterial in closed forms<sup>(44), (45)</sup>.

### References

- (1) Mitchell, M.R., Review on the Mechanical Properties of Cast Steels with Emphasis on Fatigue Behavior and Influence of Microdiscontinuities, *Trans. ASME, J. Engng. Mater. Technol.*, Oct, (1977), pp.329–343.
- (2) Murakami, Y., *Metal Fatigue: Effect of Small Defects and Nonmetallic Inclusions*, (2002), Elsevier.
- (3) Edwards, R.H., Stress Concentrations around Spherical Inclusions and Cavities, *Trans. ASME, J. Appl. Mech.*, Vol.19, No.1 (1952), pp.19–30.
- (4) Eshelby, J.D., The Determination of the Elastic Field of an Ellipsoidal Inclusion, and Related Problems, *Proceeding of the Royal Society, Ser.A*, Vol.241 (1957), pp.376–396.
- (5) Eshelby, J.D., The Elastic Field Outside an Ellipsoidal Inclusion, *Proceeding of the Royal Society, Ser.A*, Vol.252 (1959), pp.561–569.
- (6) Donnell, L.H., Stress Concentration Due to Elliptical Discontinuities in Plates under Edge Forces, *Ann. Vol. T. Von Karman, Calif. Inst. Tech.*, (1941), pp.293–309.
- (7) Nisitani, H., Approximate Calculation Method of Interaction between Notches and Its Applications, *J. Jpn. Soc. Mech. Eng.*, (in Japanese), Vol.70, No.589 (1968), pp.209–221 [*Bulletin of Jpn. Soc. Mech. Eng.*, Vol.11 (1969), pp.14–23].
- (8) Shioya, S., Tension of an Infinite Thin Plate Having Two Rigid Spherical Inclusions, *Trans. Jpn. Soc. Mech. Eng.*, (in Japanese), Vol.36 (1970), pp.886–897.
- (9) Isida, M. and Igawa, H., Some Asymptotic Behaviour and Formulate of Stress Intensity Factors for a Collinear and Parallel Cracks under Various Loadings, *Int. J. Fract.*, Vol.65 (1994), pp.247–259.
- (10) Noda, N.-A. and Matsuo, T., Analysis of a Row of Elliptical Inclusions in a Plate Using Singular Integral Equations, *Int. J. Fract.*, Vol.83 (1997), pp.315–336.
- (11) Miyamoto, H., On the Problem of the Theory of Elasticity for a Region Containing More than Two Spherical Cavities (1st Report, Theoretical Calculations), *Trans. Jpn. Soc. Mech. Eng.*, (in Japanese), Vol.23, No.131 (1957), pp.431–436.
- (12) Nisitani, H., On the Tension of an Elastic Body Having an Infinite Row of Spheroidal Cavities, *Trans. Jpn. Soc. Mech. Eng.*, (in Japanese), Vol.29, No.200, A (1963), pp.765–768.
- (13) Eubank, R.A., Stress Interference in Three-Dimensional Torsion, *Trans. ASME J. Appl. Mech.*, Vol.32, No.1 (1956), pp.21–25.
- (14) Shelly, J.F. and Yu, Y.-Y., The Effect of Two Rigid Spherical Inclusions on the Stresses in an Infinite Elastic Solids, *Trans. ASME J. Appl. Mech.*, Vol.33, No.1 (1966), pp.68–74.
- (15) Noda, N.-A., Hayashida, H. and Tomari, K., Interaction among a Row of Ellipsoidal Inclusions, *Int. J. Fract.*, Vol.102 (2000), pp.371–392.
- (16) Noda, N.-A., Ogasawara, N. and Matsuo, T., Asymmetric Problem of a Row of Revolutional Ellipsoidal Cavities Using Singular Integral Equations, *Int. J. Solids. Struct.*, Vol.40, No.8 (2003), pp.1923–1941.
- (17) Tsuchida, E. and Nakahara, I., Three-Dimensional Stress Concentration around a Spherical Cavity in a Semi-Infinite Elastic Body, *Bull. Jpn. Soc. Mech. Eng.*, Vol.13 (1970), pp.499–508.
- (18) Tsuchida, E. and Nakahara, I., Stresses in a Semi-Infinite Body Subjected to Uniform Pressure on the Surface of a Cavity and the Plane Boundary, *Bull. Jpn. Soc. Mech. Eng.*, Vol.15 (1972), pp.1–10.
- (19) Tsuchida, E., Nakahara, I. and Kodama, M., Stress Concentration around a Prolate Spheroidal Cavity in a Semi-Infinite Elastic Body under all-around Tension, *Bull. Jpn. Soc. Mech. Eng.*, Vol.25, No.202 (1982), pp.493–500.
- (20) Jasiuk, I., Sheng, P.Y. and Tsuchida, E., A Spherical Inclusion in an Elastic Half-Space under Shear, *Trans. ASME, J. Appl. Mech.*, Vol.64 (1997), pp.471–479.
- (21) Erdogan, F. and Aksogan, O., Bonded Half Planes Containing an Arbitrarily Oriented Crack, *Int. J. Solids Struct.*, Vol.10 (1974), pp.569–585.
- (22) Cook, T.S. and Erdogan, F., Stresses in Bonded Materials with a Crack Perpendicular to the Interface, *Int. J. Engng. Sci.*, Vol.10 (1972), pp.677–697.
- (23) Isida, M. and Noguchi, H., An Arbitrary Array of Cracks in Bonded Semi-Infinite Bodies under in-Plane Loads, *Trans. Jpn. Soc. Mech. Eng.*, (in Japanese), Vol.49, No.437 (1983), pp.36–45.
- (24) Willis, J.R., The Penny-Shaped Crack on an Interface,

- Q.J. Mech. & Appl. Math., Vol.25 (1972), pp.367–385.
- (25) Erdogan, F. and Arin, K., Penny-Shaped Interface Crack between an Elastic Layer and a Half-Space, *Int. J. Engng. Sci.*, Vol.10 (1972), pp.115–125.
- (26) Kassir, M.K. and Bregman, A.M., The Stress Intensity Factor for a Penny-Shaped Crack between Two Dissimilar Materials, *Trans. ASME J. Appl. Mech.*, Vol.39 (1972), pp.308–310.
- (27) Shibuya, T., Koizumi, T. and Iwamoto, T., Stress Analysis of the Vicinity of an Elliptical Crack at the Interface of Two Bounded Half-Spaces, *JSME Int. J., Ser.A*, Vol.32, No.4 (1989), pp.485–491.
- (28) Nakamura, T., Three-Dimensional Stress Fields of Elastic Interfaces Cracks, *Trans. ASME J. Appl. Mech.*, Vol.58 (1991), pp.939–946.
- (29) Yuuki, R. and Xu, J.-Q., A BEM Analysis of a Three-Dimensional Interfacial Crack of Bimaterials, *Trans. Jpn. Soc. Mech. Eng.*, (in Japanese), Vol.58, No.545, A (1992), pp.39–46.
- (30) Qin, T.Y. and Noda, N.-A., Analysis of a Three-Dimensional Crack Terminating at an Interface Using a Hypersingular Integral Equation Method, *Trans. ASME J. Appl. Mech.*, Vol.69 (2002), pp.626–631.
- (31) Qin, T.Y. and Noda, N.-A., Stress Intensity Factors of a Rectangular Crack Meeting a Bimaterial Interface, *Int. J. Solids Struct.*, Vol.40, No.10 (2002), pp.2473–2486.
- (32) Noda, N.-A., Ohzono, R. and Chen, M.-C., Analysis of an Elliptical Crack Parallel to a Bimaterial Interface under Tension, *Mechanics of Materials*, Vol.35 (2003), pp.1059–1076.
- (33) Nisitani, H., The Two-Dimensional Stress Problem Solved Using an Electric Digital Computer, *J. Jpn. Soc. Mech. Eng.*, (in Japanese), Vol.70 (1967), pp.627–632 [Bulletin of JSME, Vol.11 (1969), pp.14–23].
- (34) Noda, N.-A. and Matsuo, T., Singular Integral Equation Method in Optimization of Stress-Relieving Hole: A New Approach Based on the Body Force Method, *Int. J. Fract.*, Vol.70 (1995), pp.147–165.
- (35) Noda, N.-A. and Matsuo, T., Numerical Solution of Singular Integral Equations in Stress Concentration Problems, *Int. J. Solid Struct.*, Vol.34, No.19 (1997), pp.2429–2444.
- (36) Noda, N.-A. and Matsuo, T., Singular Integral Equation Method for Interaction between Elliptical Inclusions, *Trans. ASME J. Appl. Mech.*, Vol.65 (1998), pp.310–319.
- (37) Chen, M.-C. and Noda, N.-A., Force at a Point in the Interior of One of Two Jointed Semi-Infinite Solids, *Proceedings the 2002 Annual Meeting of JSME/MMD*, (in Japanese), No.02-05 (2002), pp.307–308; *Kikai no Kenkyu (Science of Machine)*, (in Japanese), Vol.55, No.4 (2003), pp.468–475.
- (38) Noda, N.-A. and Moriyama, Y., Stress Concentration of an Ellipsoidal Inclusion of Revolution in a Semi-Infinite Body under Biaxial Tension, *Trans. Jpn. Soc. Mech. Eng.*, (in Japanese), Vol.69, A (2003), pp.160–165.
- (39) Noda, N.-A. and Moriyama, Y., Stress Concentration of an Ellipsoidal Inclusion of Revolution in the Vicinity of a Bimaterial Interface, *Trans. Jpn. Soc. Mech. Eng.*, (in Japanese), Vol.69, No.684, A (2003), pp.1209–1215.
- (40) Noda, N.-A. and Moriyama, Y., Elastic Stress Concentration of an Ellipsoidal Inclusion of Revolution in the Vicinity of a Bimaterial Interface, *Trans. ASME, J. Engng. Mater. Technol.*, July (2004), pp.292–302.
- (41) Noda, N.-A. and Moriyama, Y., Stress Concentration of an Ellipsoidal Inclusion of Revolution in a Semi-Infinite Body under Biaxial Tension, *Arch. Appl. Mech.*, Vol.74 (2004), pp.29–44.
- (42) Nisitani, H. and Noda, N.-A., Stress Concentration of a Cylindrical Bar with a V-Shaped Circumferential Groove under Torsion, Tension or Bending, *Eng. Fract. Mech.*, Vol.20, No.5/6 (1984), pp.743–766.
- (43) Nisitani, H. and Noda, N.-A., Tension of a Cylindrical Bar Having an Infinite Row of Circumferential Cracks, *Eng. Fract. Mech.*, Vol.20, No.4 (1984), pp.675–686.
- (44) Hasegawa, H. and Sakai, T., Green's Functions for Axisymmetric Body Force Problems of Dissimilar Elastic Solids and Their Application, *Trans. Jpn. Soc. Mech. Eng.*, (in Japanese), Vol.60, No.586, A (1996), pp.1309–1515.
- (45) Hasegawa, H., Lee, V.-G. and Mura, T., Green's Functions for Axisymmetric Problems of Dissimilar Elastic Solids, *Trans. ASME. J. Appl. Mech.*, Vol.59 (1992), pp.312–320.